Cellulose (2022) 29:2175–2186
https://doi.org/10.1007/s10570-022-04450-8

ORIGINAL RESEARCH

Characterization and modeling the hygroscopic behavior of cellulose acetate membranes

Shiva Khoshtinat · Valter Carvelli · Claudia Marano

Received: 18 November 2021 / Accepted: 20 January 2022 / Published online: 7 February 2022

Abstract Exploiting materials with the ability to respond to the environmental stimuli is experiencing an enormous research interest. In particular, polymers that are sensitive to the changes of humidity levels attract great attention as self-actuators. The sensitivity of these materials to the level of moisture is expressed by their hygroscopic properties, namely, the coefficient of hygroscopic expansion. In this context, this study details the effect of moisture absorption on cellulose acetate membranes, as potential material for humidity-responsive self-actuators. The aim is two-fold. The first deals with the evaluation of the coefficient of hygroscopic expansion (α) through the determination of the absorbed moisture concentration at saturation (C_{sat}) and the relevant moisture absorption induced strain (ε_{hygro}). The second assesses the accuracy of a finite element modeling in describing the coupling of moisture absorption in cellulose acetate membranes and the corresponding dimensional variation, using the material properties experimentally measured. The experimentally measured C_{sat} and ε_{hygro} resulted a non-linear dependency on relative humidity. Also the coefficient of hygroscopic expansion ($\alpha = C_{sat}/\varepsilon_{hygro}$) resulted to have a non-linear dependency on the relative humidity, as well. By this input, numerical simulations were performed for different relative humidity levels, showing accurate description of experimental data.

Keywords Humidity responsive materials · Cellulose acetate · Coefficient of hygroscopic expansion · Finite element modeling · Thermomechanical analysis

Introduction

Hygroscopic expansion, which is defined as dimensional variation due to moisture absorption, can be a double-edged sword. For decades, the hygroscopic behavior of materials has been considered a drawback that influences product performance (Wong 2010). In recent years, the application of hygroscopic materials as self-actuator or humidity responsive products has been continuously exploited in different industries. The products integrating this feature have ranged from the small scale of humidity-sensitive self-actuators for

S. Khoshtinat · C. Marano (✉)
Department of Materials, Chemistry and Chemical Engineering, Giulio Natta" Politecnico di Milano, Piazza Leonardo Da Vinci 32, 20133 Milan, Italy
e-mail: claudia.marano@polimi.it

S. Khoshtinat
e-mail: shiva.khoshtinat@polimi.it

V. Carvelli
Department of Architecture, Built Environment and Construction Engineering Politecnico Di Milano, Piazza Leonardo da Vinci 32, 20133 Milan, Italy
e-mail: valter.carvelli@polimi.it

sensor application (Taccola et al. 2015; Heibeck et al. 2015; Rivadeneyra et al. 2021) to the larger scale of environmentally responsive building facades (Menges and Reichert 2015; Bridgens et al. 2017; Abdelmohsen 2019). Moreover, some wearable textile (Wang et al. 2017) and energy harvesting application (Chen et al. 2014, 2015) have employed this feature.

Most of these research studies consider a bi-layered composite that couples a hygroscopic material layer with a layer of a non-hygroscopic material. These studies exploit the different dimensional variation of the two layers induced by a change in the environment humidity to obtain a self-actuator device. The actuation in these bi-layered composites is a function of changes in environmental conditions (relative humidity and/or temperature), of the device geometry (layers thickness), as well as the intrinsic properties of each layer materials.

For a proper design of these actuators, the most important material property to be determined is the hygroscopic expansion coefficient (α). α is defined as the ratio of the relative linear expansion induced in a dried material by moisture absorption (ε_{hygro}), and the moisture concentration at saturation C_{sat}, namely $\alpha = \frac{\varepsilon_{hygro}}{C_{sat}}$ (Wong 2010). In this definition, ε_{hygro}, often referred to as the hygroscopic strain, and C_{sat} are estimated with respect to the dry condition ($\varepsilon_{hygro} = \frac{L_{sat}-L_{dry}}{L_{dry}}, C_{sat} = \frac{M_{sat}-M_{dry}}{V_{dry}}$),where, L, M, and V are the length, mass and volume of the body under consideration, and the subscripts '*sat*' and '*dry*' refer to saturation and dry conditions, respectively.

Different experimental methods have been used for the evaluation of a material coefficient of hygroscopic expansion. Some methods are based on a direct warpage measurement of bi-material beams, some on a direct strain measurement using Moiré interferometry (Stellrecht et al. 2003; Changsoo Jang et al. 2010) or Digital image correlation (DIC) analysis (Changsoo Jang et al. 2010). In some works, volume variations induced by material drying have been evaluated by Archimedes Principle (Wong 2010), while other researches exploited a parallel Thermomechanical (TMA) and Thermogravimetric analysis (TGA) (Jiang Zhou et al. 2005; Shirangi et al. 2008, 2009b, a; Park et al. 2009; Zhang et al. 2010). TGA is the most used technique for the determination of C_{sat}. It measures the weight loss of a specimen, preliminarily saturated at a certain value of relative humidity and temperature, during the desorption process, till dry condition is reached.

Each of the above mentioned methods or techniques has its own limits to some extent. For instance, warpage measurement of bi-material beams is not suitable for the materials that show a non-reversible hygroscopic expansion or bi-layered composites in which the moisture absorption can cause micro-cracks or delamination between two layers (Jiang Zhou et al. 2005; Shirangi et al. 2009b, a). The parallel TMA/TGA method is not suitable when the drying temperature passes the glass transition temperature of the material (Jiang Zhou et al. 2005; Shirangi et al. 2008, 2009b, a; Park et al. 2009; Zhang et al. 2010). The strain measurement in thin films based on Moiré interferometry method needs meticulous attention to the applied external force, as it can cause unforeseen deformation (Stellrecht et al. 2003; Changsoo Jang et al. 2010). It has to be noticed that, irrespective of the adopted method, both the concentration at saturation (C_{sat}) and the hygroscopic strain (ε_{hygro}) are mostly measured during a moisture desorption process, that is by comparing the initial (humid) and the final (dry) values of a body mass and dimensions.

Given the complexity of moisture absorption/desorption processes, overlapping data from experiments based on different techniques based on different assumptions, lead often to measurements with not negligible errors. For example, the mentioned methods assume identical hygroscopic behavior during the absorption and desorption process and evaluate the diffusion coefficient during the desorption process, despite it has been demonstrated the diffusion kinetics during moisture absorption and moisture desorption are completely different (Crank 1979; De Wilde and Shopov 1994; Mensitieri and Scherillo 2012). Another approximation is the linear relation between hygroscopic strain and moisture concentration with relative humidity, so that the coefficient of hygroscopic expansion results to be constant and independent of relative humidity (Stellrecht et al. 2003; Jiang Zhou et al. 2005; Shirangi et al. 2008, 2009b, a; Park et al. 2009; Changsoo Jang et al. 2010; Zhang et al. 2010). These two assumptions can lead to a considerable discrepancy between the measurements and real hygroscopic behavior, especially, for highly hygroscopic materials during the absorption. These hypotheses might be suitable for materials having a very slow absorption process, getting the

concentration at saturation after several months or even years. While, for highly hygroscopic materials, reaching the saturation in less than an hour, these assumptions are questionable. For highly hygroscopic materials, considerable attention must be paid to the measurement of the hygroscopic strain by Thermomechanical Analysis (TMA) using membranes. The measurement of the dimensional variation through the thickness can lead to poor accuracy in the obtained values for hygroscopic strains.

To overcome some of the mentioned drawbacks, in this study, the concentration at saturation of a cellulose acetate has been evaluated by direct gravimetric measurements of membranes during the absorption process. Despite this technique is time consuming, it is more suitable for highly hygroscopic materials having a different absorption and desorption kinetics (Crank and Park 1951; Crank 1953; Alfrey Jr et al. 1966; Roussis 1981; De Wilde and Shopov 1994; Mensitieri and Scherillo 2012).

The dimensional variation induced in a dried membrane is independent of both moisture absorption and diffusion kinetics; when the material reaches a moisture concentration at saturated state. Therefore, the hygroscopic strain can still be determined referring to the desorption process by Thermomechanical analysis (TMA) using a proper tool, as presented in this study. Dealing with very thin membranes (thickness lower than 500 μm), a tensile loading configuration was adopted using the film/fiber probe of a Thermomechanical Analyzer.

The obtained results, detailed in the experimental section, were used to define a correlation between the hygroscopic strain (ε_{hygro}) and the concentration at saturation state (C_{sat}) with the environment Relative humidity (RH). The experimental data of moisture concentration at saturation and hygroscopic strain have been used, among the other inputs, for the finite element modeling of coupled moisture diffusion and hygroscopic expansion. The numerical model has accurately predicted the effect of moisture absorption on the mechanical deformation of the considered cellulose acetate membranes.

Material and membrane preparation

Cellulose acetate (CA) powder (53.3% acetylation) was kindly provided by Mazzucchelli 1849 S.p.A. As it was described in a previous study (Khoshtinat et al. 2021), a 20% w/w solution of Cellulose Acetate (CA) in ethyl lactate (purity ≥ 98%, purchased from Sigma-Aldrich) was first prepared (Fig. 1a) for the production of cellulose acetate membranes. A layer of about 500 μm thickness of the solution was casted by K Control Coater at room temperature. Drying of CA film was carried out in several steps (Fig. 1b) to optimize the whole evaporation of the solvent (Khoshtinat et al. 2021). Membranes with a thickness ranging from 66 ± 1.5 to 70 ± 4.5 μm were obtained (measured by micrometer). Thicker membranes with a thickness between 145 ± 2 and 200 ± 10.5 μm have been obtained repeating the same procedure using a dried CA membrane as substrate in the solution pouring process instead of a glass plate. The CA membranes, pealed from the glass substrate, were then dried in an oven (Mazzali Thermair) for 24 h at 125 °C to ensure the complete evaporation of the residual solvent, if any. During the drying process, the membrane was placed between two metal frames to allow equal evaporation at both surfaces. Specimens were cut from the central part of each membrane at least at a distance of 1 cm from the metal frames: this area was considered free from any clamping system influence and thus eligible for obtaining specimen for moisture absorption and membrane expansion measurements. Specimens for gravimetric measurements, with dimensions of 30 × 30 mm^2, and for Thermomechanical Analysis, with dimensions of 20 × 4 mm^2, were respectively punched and cut from the obtained films (Fig. 1c).

Experimental procedures and measurements

Concentration at saturation

The concentration at saturation (C_{sat}) has been determined during the absorption process via gravimetric measurements. Most of these measurements are reported in (Khoshtinat et al. 2021), where data of CA membrane mass variation in time, monitored at 25 ± 1 °C and at different values of relative humidity (RH in the range 21 ÷ 53%), are detailed. In the present work new tests have been performed at higher relative humidity values, up to 76%. The 30 mm × 30 mm (900 mm^2) specimens had been previously dried at 125 °C for 24 h in an oven (Mazzali Thermair), then

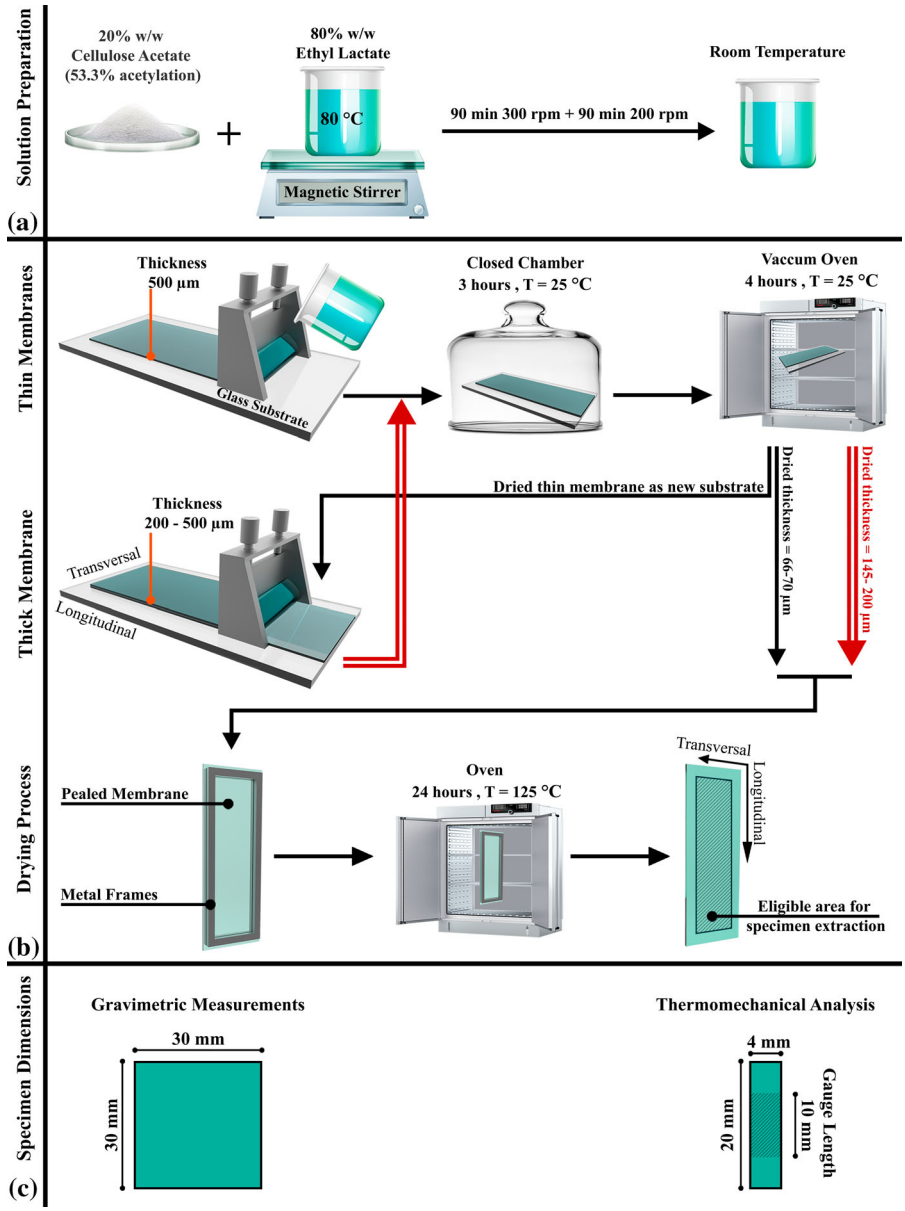

Fig. 1 Schematic representation of: **a** solution preparation procedure; **b** membrane production and drying process; **c** specimen dimensions

placed and kept for 2 h at the room temperature in a desiccator before performing moisture absorption measurements. For weight measurement, an AS310.R2—RADWAG balance with a limit of readability of 0.1 mg was used. As reported previously (Khoshtinat et al. 2021) the "*variable surface concentration*" model was adopted to describe the sigmoidal moisture absorption of the cellulose acetate membrane and to predict the concentration at saturation (C_{sat}) for different values of relative humidity. Figure 2 summarizes the obtained C_{sat} values (at least 3 measurements) for different levels of Relative humidity (RH) by the best fitting of the variable surface concentration model interpolating the experimental data.

Figure 2 shows that the hypothesis of a linear dependence of C_{sat} on the relative humidity ($C_{sat} = S \times p_{sat} \times RH$), where p_{sat} and S are the water partial

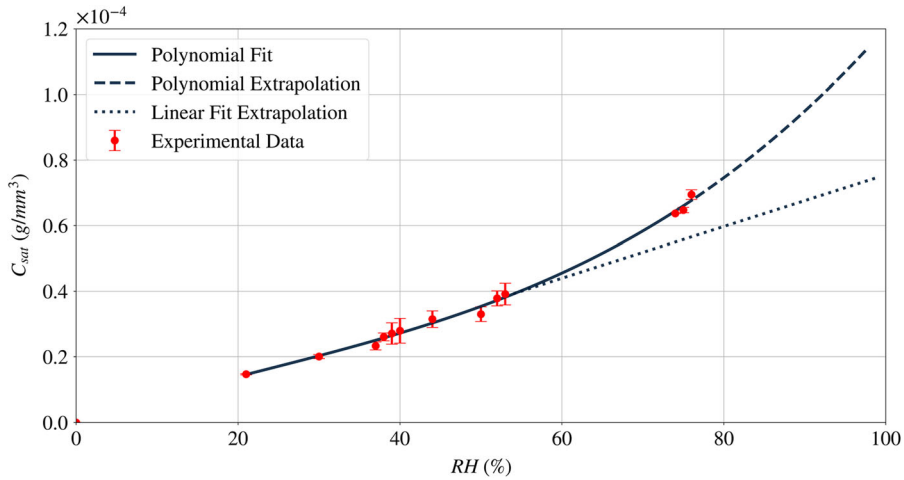

Fig. 2 Average moisture concentration at saturation (C_{sat}) as a function of relative humidity (RH) (bars represent the standard deviation)

vapor pressure at saturation and the water vapor solubility, respectively) (Fan et al. 2009; Wong 2010), is valid in a limited range of RH. As reported (Lauri et al.; Shrestha et al. 2017), cellulose-based materials deviate from this linear prediction, showing a considerable discrepancy starting from a certain level of relative humidity. This RH level (about 53% in this study), as well as the increase of the slope of the C_{sat} vs. RH curve, depends on several parameters, such as: the type of cellulose and its degree of crystallinity, the acetylation process, and the presence of plasticizers or other chemical elements (Gibbons 1953).

For the considered cellulose acetate, the concentration at saturation at a relative humidity of 74–76% is about 1×10^{-5} g mm^{-3} higher than the value extrapolated from the linear fit of the experimental data below 53% of relative humidity. The experimental data show a trend similar to that of other cellulose based materials (Lauri et al.; Shrestha et al. 2017) and thus they have been interpolated in the same way with a polynomial function. Assuming $C_{sat} = 0$ g mm^{-3} for $RH = 0\%$, the concentration at saturation was fitted with a third-order polynomial function (Eq. 1), with R^2 of 0.996.

$$C_{sat} = 1.19 \times 10^{-10} \times RH^3 - 7.97 \times 10^{-9} \times RH^2 + 8.09 \times 10^{-7} \times RH \quad (1)$$

Hygroscopic strain

The hygroscopic strain (ε_{hygro}) was determined by Thermomechanical Analysis. A Discovery TMA 450 (TA instruments®) with the film/fiber probe was used. To assess the anisotropic behavior of the CA membrane due to the manufacturing process, specimens were cut both in the longitudinal and transversal directions with respect to the K Coater control blade movement direction: at least three specimens for each direction were tested. The specimens were preconditioned at 25 °C and at different levels of relative humidity (RH = 31 ÷ 76%) for at least 24 h, to reach saturation conditions in a climatized cabinet. Since the mounting of the specimen between the jaws took some minutes and the material may have desorb moisture in this period, each specimen was mounted between the jaws and kept one more hour inside the climatized chamber to regain the lost moisture, if any. Then, it was moved to TMA. The whole process of specimen moving and closing the cell of TMA took less than 20 s. Standard ASTM E831-6 which refers to test using expansion probes, foresees the application of a force between 1 and 100 mN to guarantee the contact of the specimen and the probe. In this work, the applied force was varied in each test to have an applied pre-stress of 1 MPa, which causes a negligible mechanical deformation during the whole test (see Fig. 3) and as expected considering the experimental values of the Young's modulus of 1.1 ± 0.09 and 0.7 ± 0.09 GPa for the cellulose acetate measured by

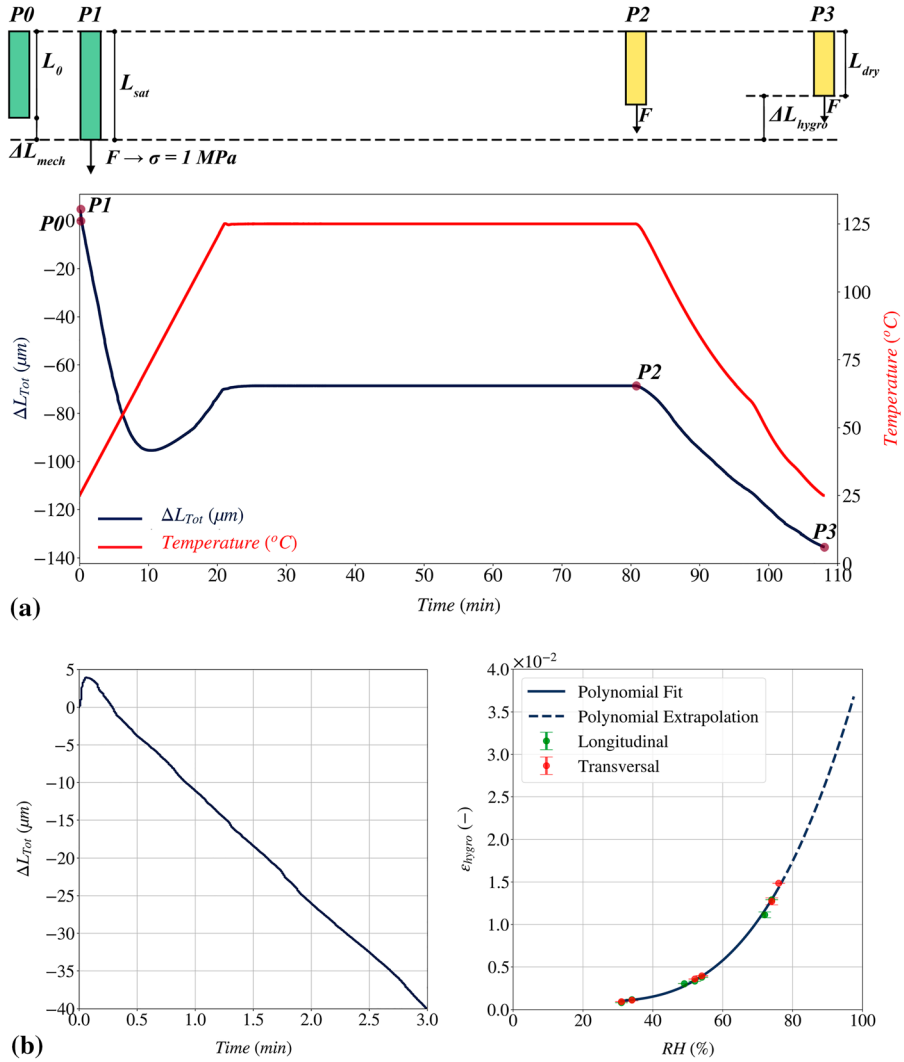

Fig. 3 Thermomechanical Analysis procedure: **a** thermal profile and relative dimensional change vs. time, **b** dimension variation recorded at short time, **c** hygroscopic strain evaluated by Thermomechanical Analysis (bars represent data semi-dispersion for 3 measurements) and the polynomial best fitting

uniaxial tensile test (strain rate 6×10^{-3} 1/min) in two considerably different conditions, namely: room temperature (25 ± 1 °C) and RH = 35–41%; immersed in water.

All the TMA tests started at 25 °C, that is the temperature CA moisture saturation was reached for each level of relative humidity. The TMA test procedure was:

(i) Measurement of the initial length (L_0);
(ii) Application of the force to get a pre-stress of 1 MPa to keep the specimen in tension through the whole process;
(iii) Heating at 5 °C/min from 25 to 125 °C to allow moisture desorption;
(iv) Keeping isothermal conditions at 125 °C of one hour to ensure the complete specimen drying;
(v) Cooling at 5 °C/min from 125 to 25 °C to recover the thermal expansion.

The specimen dimensions (length, width and thickness) have been measured both before (humid condition) and after the TMA test (dry condition).

For the sake of brevity, Fig. 3 shows experimental data and its analysis for one test (specimen

conditioned at $RH = 75\%$ and T = 25 °C). Figure 3(a) depicts the thermal profile together with the total variation of the specimen length ΔL_{Tot} and a sketch reproducing the specimen in each step of the test. The specimen dimensional change is the result of the superposition of three phenomena, and thus it is the sum of three components (Eq. 2), namely the mechanical (ΔL_{mech}), the thermal (ΔL_{therm}), and the hygroscopic (ΔL_{hygro}) one.

$$\Delta L_{Tot} = \Delta L_{mech} + \Delta L_{therm} + \Delta L_{hygro} \quad (2)$$

In Fig. 3a, P0 indicates the starting condition, while *P1* shows the sudden elongation in the early stage of the test, due to the applied force ($F \rightarrow \sigma = 1MPa$). Figure 3b provides an enlargement of Fig. 3a in this stage. The applied force caused a mechanical elongation of about 4 µm for the considered specimen (corresponding to the mechanical strain of 0.03%).

Starting with the heating ramp from *P1*, one would expect an increase in the length due to thermal expansion, while a decrease of length can be observed. This is consequence of the hygrothermal deformation, which is the superposition of a thermal expansion due to the increase of the temperature and a hygroscopic shrinkage due to the moisture desorption. For the considered *RH* saturation levels, the hygroscopic contraction is much higher than the thermal expansion occurring in the first 15 min of the test. This trend continues up to a temperature of about 85 °C, at which the specimen shrank of about 100 µm with respect to its *P1* length. Afterwards the specimen length slightly increases till the temperature reaches the set point of 125 °C, suggesting that the thermal expansion is overtaking the hygroscopic shrinkage.

During the isothermal step of one hour at 125 °C, a negligible variation of elongation can be observed. These results suggest that the specimen is completely dry and the applied force does not induce any creep in the specimen. At the end of this step (*P2*), the cooling to 25 °C of the completely dry specimen induces only a thermally contraction. The length variation measured in this step is thus ΔL_{therm}. *P3* indicates the dry specimen equilibrated at 25 °C.

Since, in this experimental procedure, the whole moisture desorption occurs under the application of a mechanical load, the length of specimen at *P1* has to be considered as the length in saturated condition (L_{sat}), and the length at *P3* as the length in dry condition (L_{dry}).

Figure 3c shows the evaluated hygroscopic strain ($\varepsilon_{hygro} = (L_{humid} - L_{dry}) / L_{dry}$) as a function of relative humidity for tested specimens extracted in the two directions. No orientation dependency has been observed, which confirms the isotropy of the membrane. As observed on *RH* dependency of CA moisture concentration at saturation (Fig. 2), the hygroscopic strain experiences a sharp increase when relative humidity exceeds 53%. In analogy to C_{sat} (Fig. 2), the trend of hygroscopic strain (ε_{hygro}) plotted versus relative humidity has been fitted by a third order polynomial function (Eq. 3), with R^2 of 0.997.

$$\varepsilon_{hygro} = 8.03 \times 10^{-8} \times RH^3 - 5.14 \times 10^{-6} \times RH^2 + 1.16 \times 10^{-4} \times RH \quad (3)$$

Coefficient of hygroscopic expansion

The coefficient of hygroscopic expansion (α) has been estimated considering the two functions describing the concentration at saturation (C_{sat}) and the hygroscopic strain (ε_{hygro}) in relation to the relative humidity (Eq. 1 and 3). The difference between the evolution with the relative humidity of the moisture concentration at saturation and of the relative induced hygroscopic strain (Fig. 4a) can be explained, from a physical point of view, with the porosity of the membrane as also explained in (Wong 2010). At relative humidity levels lower than 40%, the moisture absorbed by the material just fills the membrane nanopores (Xuejun Fan 2008). No water molecules interaction with the hydroxyl groups of the CA molecular chains which are responsible for the material expansion occurs. This interaction, instead, takes place at higher values of *RH*.

According to definition in introduction, the coefficient of hygroscopic expansion (α) is reported as the ratio between the hygroscopic strain and the relevant moisture concentration at saturation (Eq. 4).

$$\alpha = \frac{\varepsilon_{hygro}}{C_{sat}} = \frac{803 \times RH^2 - 51400 \times RH + 1.16 \times 10^6}{1.19 \times RH^2 - 79.7 \times RH + 8090} \quad (4)$$

As a common assumption, for many materials the hygroscopic expansion is considered a single value, that can be evaluated as the slope of the line fitted to

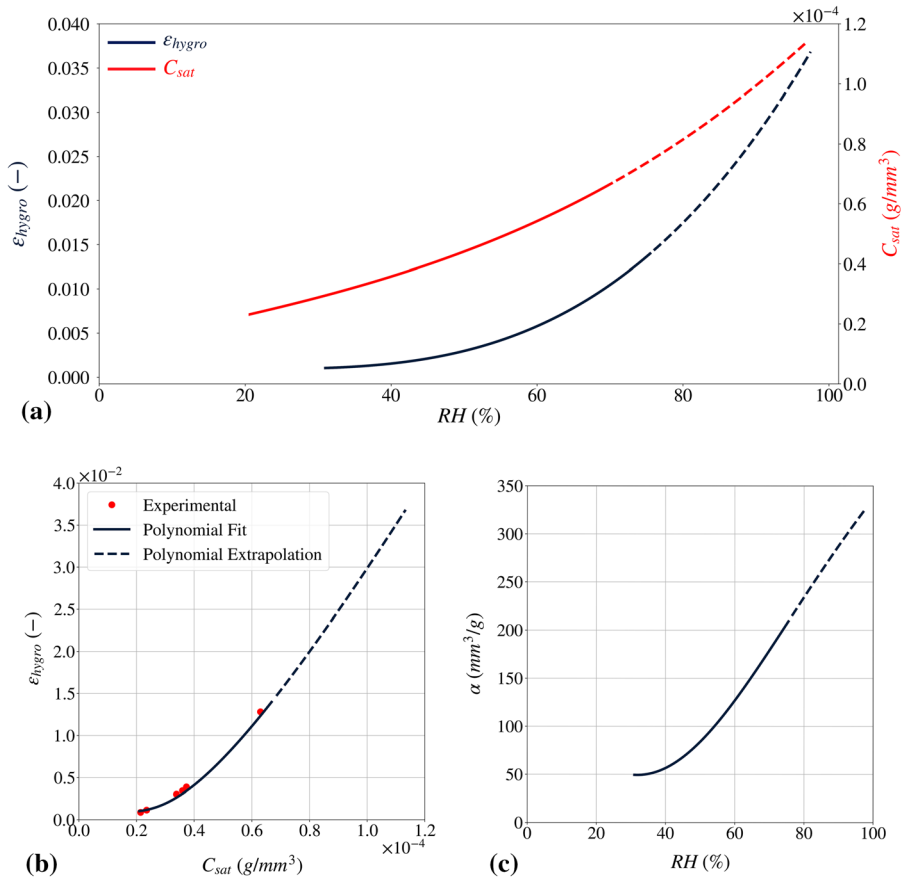

Fig. 4 **a** Relative humidity dependence of hygroscopic strain and concentration at saturation state as predicted by Eq. 1 and 3; **b** hygroscopic strain as a function of moisture concentration at saturation; **c** coefficient of hygroscopic expansion (α) as function of relative humidity

the graph of hygroscopic strain (ε_{hygro}) as the function of relevant concentration at saturation (C_{sat}), intercepting at zero (Wong 2010). Figure 4b depicts the mentioned graph for our study, using Eq. 1 and 3. It also demonstrates that the experimental data available for both gravimetric and thermomechanical analysis (C_{sat} and ε_{hygro}) for the same level of relative humidity are in a good agreement with polynomial functions (Eq. 1 and 3) that have been obtained, separately. Using the common approach in the literature of linear fit to the curve in Fig. 4b, intercepting at zero, provides the constant value of α = 138 mm^3/g (R^2 of about 0.89). Figure 4c, on the other hand, shows the nonlinear variation of α, for the considered cellulose acetate, by plotting Eq. 4 as the function of relative humidity. The trend of evolution of α as the function of relative humidity in this study is similar to the behavior detailed by Teverovsky (Teverovsky 2002).

Finite element modeling

For the prediction of the strain induced by moisture absorption, finite element simulations by COMSOL Multiphysics® 5.6 were performed. A multiphysics approach coupling transport of diluted species and solid mechanic has been used to predict the induced hygroscopic strain. To reduce the computational time, a time-dependent analysis for absorbed moisture concentration and then a stationary analysis for mechanical response have been implemented.

A 3D prismatic geometry has been used to discretize each specimen with the dimensions of the dry condition. The dry specimen length, width and thickness (measured at the end of the thermomechanical analysis test) have been used to discretize one fourth of the prism ($\frac{L_{dry}}{2} \times \frac{W_{dry}}{2} \times h_{dry}$) exploiting the symmetries to reduce the calculation time (Fig. 5). A

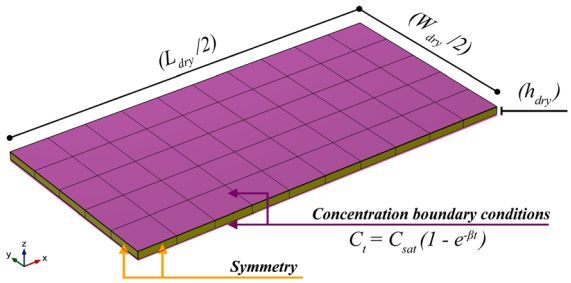

Fig. 5 Schematic representation of the finite element model

user-defined material has been adopted to apply the intrinsic properties of the cellulose acetate in this study. The physical and mechanical properties defined for the cellulose acetate in dry condition were: density 1.3×10^{-4} (g /mm^3) (Wypych 2016), Young's modulus 1.1 GPa and Poisson's ratio 0.39 (Wypych 2016). A relaxation factor of $\beta = 0.026$ s^{-1} and a diffusion coefficient of $D = 3.35 \times 10^{-06}$ mm^2/s have been used (Khoshtinat et al. 2021). The coefficient of hygroscopic expansion (α) has been defined as a function of relative humidity (*RH*) according to Eq. 4.

The adopted time-dependent model for the non-Fickian behavior is the one detailed in the previous work (Khoshtinat et al. 2021). The concentration at saturation (C_{sat}) has been defined as function of Relative humidity (*RH*) according to Eq. 1, and has been applied to the specimen top and bottom faces.

A user-controlled, general physics swept mesh with quadrilateral face through a straight-line path has been applied from one lateral surface to the other, which generates a discretized volume by $10 \times 5 \times 10$ hexahedral elements (total of 500 elements exploiting symmetries). After performing the simulation, the length at humid condition (direction X) have been considered to estimate the induced hygroscopic strain.

Numerical results and discussion

The numerical analysis results allowed to discuss two aspects:

- The accuracy of the finite element model comparing the predicted numerical hygroscopic strains (ε_{hygro}) to experimental measurements;
- The inappropriateness of the assumption of constant value for the coefficient of hygroscopic expansion (Wong 2010) comparing the numerical results to those get with the non-linear relative humidity dependency (Eq. 4).

For the comparison purpose, the experimental results obtained from specimens conditioned at *RH* levels of 31, 52 and 74% were considered. The dimensions of the specimens at dry conditions (measured at the end of TMA tests) were used as input to create the solid model of each numerical analysis (Table 1). Two sets of numerical simulation have been done: first, using the dependency of the hygroscopic expansion coefficient on the level of relative humidity as calculated by Eq. 4, considering a constant value of $\alpha = 138$ mm^3/g, from Fig. 4b.

The comparison between the predicted hygroscopic strain by the finite element simulation for each humidity level and the experimental data (Fig. 6) shows, as expected, very good agreement. This indicates that the coupling of non-Fickian moisture diffusion and the corresponding induced mechanical deformation due to the absorption is able to provide the value of final induced hygroscopic expansion with a good level of accuracy.

The comparison between simulation of hygroscopic expansion by constant (138 mm^3/g) and *RH* dependent coefficient of hygroscopic expansion (α) is detailed in Fig. 6. As expected, by considering a constant value of α, the hygroscopic strain predicted by the model shows a steady increase by the increase of the relative humidity, which leads to a considerable discrepancy to the experimental measurements. The predicted hygroscopic strain simulated by the constant α coincides with the real value in just one level of relative humidity (RH = 62%), where the α calculated by Eq. 4 is equal to the evaluated constant α (138 mm^3/g). All the other simulations performed with a constant value of α lead to an overestimation or an underestimation of the hygroscopic strain. This comparison demonstrates that the effect of relative humidity on the coefficient of hygroscopic expansion (α) is not negligible. Moreover, it highlights that for a highly hygroscopic material, such as cellulose acetate, the coefficient of hygroscopic expansion (α) cannot be considered neither constant, nor linearly dependent on relative humidity.

Table 1 Input parameters for finite element simulations

Condition	L_{dry} (mm)	W_{dry} (mm)	h_{dry} (mm)	C_{sat} (*) (g mm^{-3})	α (*) (mm^3 g^{-1})
RH = 31%	11.054	3.9	0.116	2.1×10^{-5}	50
RH = 52%	11.025	4	0.104	3.73×10^{-5}	92
RH = 74%	11.886	3.8	0.110	6.44×10^{-5}	201

(*)C_{sat} and α are calculated by Eq. 2 and 5, respectively

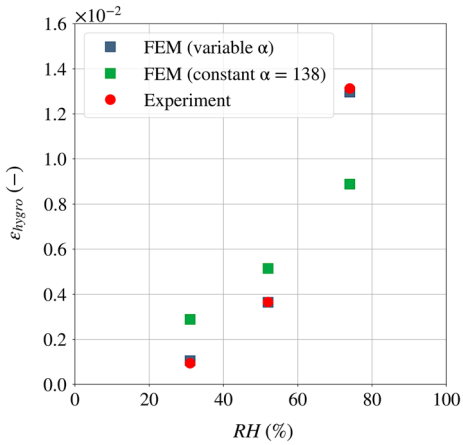

Fig. 6 Comparison of experimental and finite element predicted hygroscopic strains, assuming value or a RH dependent coefficient of hygroscopic expansion

Conclusions

The relative humidity dependence of the coefficient of hygroscopic expansion (α) of a cellulose acetate (53.3% of acetylation) has been evaluated at constant temperature of 25 ± 1 °C. The concentration at saturation (C_{sat}) at room temperature and different relative humidity levels (RH = 21 ÷ 76%) has been determined via gravimetric measurements performed during moisture absorption. The hygroscopic strain (ε_{hygro}) of pre-conditioned specimens (T = 25 ± 1 °C, RH = 31 ÷ 76%) has been measured during the desorption via Thermomechanical analysis (TMA). Despite the common assumptions, at constant temperature (25 ± 1 °C), concentration at saturation (C_{sat}) and hygroscopic strain (ε_{hygro}) did not show a linear relation with relative humidity. Nonlinear dependencies have been observed, fitting by third order polynomials, resulting in nonlinear coefficient of hygroscopic expansion with the relative humidity.

The experimental results for moisture concentration at saturation (C_{sat}) and hygroscopic strain (ε_{hygro}) have been considered as input of a finite element model coupling moisture diffusion and hygroscopic expansion. The simulations were performed for different relative humidity levels. The comparison between the FE simulation and experimental data confirmed the validity of the simulation method, which must consider the proper nonlinear dependency of the coefficient of hygroscopic expansion on the relative humidity. The knowledge collected by the present study is the background for further investigation aiming to the development of a self-actuator humidity responsive layered material exploiting the obtained features of cellulose acetate. This is also the proper context to investigate the response to cyclic variations of the humidity.

Authors' contributions SK: Investigation; Conceptualization, Methodology, Data curation, Formal analysis, Validation, Writing–original draft; VC: Investigation; Conceptualization, Supervision; Writing–review & editing CM: Investigation; Conceptualization, Supervision, Methodology, Validation, Writing–review & editing.

Funding No funding was received for conducting this study.

Data availability All the data has been reported as *Online Resource.*

Code availability Software application or custom code are available on request.

Declarations

Conflicts of interest The authors declare that they have no known competing financial interests or personal relationships that could have appeared to influence the work reported in this paper.

Consent to participate All authors gave explicit consent to participate.

Consent for publication All authors gave explicit consent to submit.

References

Abdelmohsen S (2019) HMTM: Hygromorphic-Thermobimetal Composites as a Novel Approach to Enhance Passive Actuation of Adaptive Façades. 18th CAAD Futur 2019 Int Conf

Alfrey T Jr, Gurnee EF, Lloyd WG (1966) Diffusion in glassy polymers. J Polym Sci Part c: Polym Symposia. 12:249–261

Bridgens B, Holstov A, Farmer G (2017) Architectural application of wood-based responsive building skins. In: In Proceedings of the 12th International Conference on Advanced Building Skins. pp 2–3

Chen X, Mahadevan L, Driks A, Sahin O (2014) Bacillus spores as building blocks for stimuli-responsive materials and nanogenerators. Nat Nanotechnol 9:137–141. https://doi.org/10.1038/nnano.2013.290

Chen X, Goodnight D, Gao Z et al (2015) Scaling up nanoscale water-driven energy conversion into evaporation-driven engines and generators. Nat Commun 6:7346. https://doi.org/10.1038/ncomms8346

Crank J (1953) A theoretical investigation of the influence of molecular relaxation and internal stress on diffusion in polymers. J Polym Sci 11:151–168. https://doi.org/10.1002/pol.1953.120110206

Crank J (1979) The mathematics of diffusion. Oxford University Press

Crank J, Park GS (1951) Diffusion in high polymers: some anomalies and their significance. Trans Faraday Soc 47:1072. https://doi.org/10.1039/tf9514701072

De Wilde WP, Shopov PJ (1994) A simple model for moisture sorption in epoxies with sigmoidal and two-stage sorption effects. Compos Struct 27:243–252. https://doi.org/10.1016/0263-8223(94)90085-X

Fan XJ, Lee SWR, Han Q (2009) Experimental investigations and model study of moisture behaviors in polymeric materials. Microelectron Reliab 49:861–871. https://doi.org/10.1016/j.microrel.2009.03.006

Gibbons GC (1953) 12—the moisture regain of methylcellulose and cellulose acetate. J Text Inst Trans 44:T201–T208. https://doi.org/10.1080/19447025308659739

Heibeck F, Tome B, Della Silva C, Ishii H (2015) uniMorph:Fabricating Thin-Film Composites for Shape-Changing Interfaces. In: Proceedings of the 28th Annual ACM Symposium on User Interface Software & Technology. ACM, New York, NY, USA, pp 233–242

Jang C, Yoon S, Han B (2010) Measurement of the Hygroscopic Swelling Coefficient of Thin Film Polymers Used in Semiconductor Packaging. IEEE Trans Components Packag Technol 33:340–346. https://doi.org/10.1109/TCAPT.2009.2038366

Jiang Z, Lahoti SP, Sitlani MP, et al (2005) Investigation of non-uniform moisture distribution on determination of hygroscopic swelling coefficient and finite element modeling for a flip chip package. In: EuroSimE 2005. Proceedings of the 6th International Conference on Thermal, Mechanial and Multi-Physics Simulation and Experiments in Micro-Electronics and Micro-Systems, 2005. IEEE, pp 112–119

Khoshtinat S, Carvelli V, Marano C (2021) Moisture absorption measurement and modelling of a cellulose acetate. Cellulose 28:9039–9050. https://doi.org/10.1007/s10570-021-04114-z

Lauri VAL (2017) Thaddeus R, Maloney C Changes in the hygroscopic behavior of cellulose due to variations in relative humidity. Cellulose 25:87–104

Menges A, Reichert S (2015) Performative Wood: Physically Programming the Responsive Architecture of the HygroScope and HygroSkin Projects. Archit Des 85:66–73. https://doi.org/10.1002/ad.1956

Mensitieri G, Scherillo G (2012) Environmental Resistance of High Performance Polymeric Matrices and Composites. In: Wiley Encyclopedia of Composites. John Wiley & Sons, Inc., Hoboken, NJ, USA

Park S, Haojun Zhang, Xin Zhang, et al (2009) Temperature dependency of coefficient of hygroscopic swelling of molding compound. In: 2009 59th Electronic Components and Technology Conference. IEEE, pp 172–179

Rivadeneyra A, Marín-Sánchez A, Wicklein B et al (2021) Cellulose nanofibers as substrate for flexible and biodegradable moisture sensors. Compos Sci Technol 208:108738. https://doi.org/10.1016/j.compscitech.2021.108738

Roussis PP (1981) Diffusion of water vapour in cellulose acetate: 1. Differential transient sorption kinetics and equilibria. Polymer (guildf) 22:768–773. https://doi.org/10.1016/0032-3861(81)90012-4

Shirangi MH, Wunderle B, Wittler O et al (2009b) Modeling cure shrinkage and viscoelasticity to enhance the numerical methods for predicting delamination in semiconductor packages. 2009 10th Int Conf Therm Mech Multi-Physics Simul Exp Microelectron Microsystems. EuroSimE 2009:1–8. https://doi.org/10.1109/ESIME.2009.4938412

Shirangi H, Auersperg J, Koyuncu M, et al (2008) Characterization of dual-stage moisture diffusion, residual moisture content and hygroscopic swelling of epoxy molding compounds. In: EuroSimE 2008 - International Conference on Thermal, Mechanical and Multi-Physics Simulation and Experiments in Microelectronics and Micro-Systems. IEEE, pp 1–8

Shirangi MH, Muller WH, Michel B (2009a) Effect of nonlinear hygro-thermal and residual stresses on the interfacial fracture in plastic IC packages. In: 2009 59th Electronic

Components and Technology Conference. IEEE, pp 232–238

Shrestha S, Diaz JA, Ghanbari S, Youngblood JP (2017) Hygroscopic Swelling Determination of Cellulose Nanocrystal (CNC) Films by Polarized Light Microscopy Digital Image Correlation. Biomacromol 18:1482–1490. https://doi.org/10.1021/acs.biomac.7b00026

Stellrecht E, Han B, Pecht M (2003) Measurement Of The Hygroscopic Swelling Coefficient In Mold Compounds Using Moire InterferometRY. Exp Tech 27:40–44. https://doi.org/10.1111/j.1747-1567.2003.tb00122.x

Taccola S, Greco F, Sinibaldi E et al (2015) Toward a New Generation of Electrically Controllable Hygromorphic Soft Actuators. Adv Mater 27:1668–1675. https://doi.org/10.1002/adma.201404772

Teverovsky A (2002) Moisture characteristics of molding compounds in PEMs

Wang W, Yao L, Cheng C-Y et al (2017) Harnessing the hygroscopic and biofluorescent behaviors of genetically tractable microbial cells to design biohybrid wearables. Sci Adv 3:e1601984. https://doi.org/10.1126/sciadv.1601984

Wong CP (2010) Moisture Sensitivity of Plastic Packages of IC Devices. Springer, US, Boston, MA

Wypych G (2016) Handbook of Polymers: Second Edition. Elsevier Inc.

Xuejun Fan (2008) Mechanics of moisture for polymers: Fundamental concepts and model study. In: EuroSimE 2008 - International Conference on Thermal, Mechanical and Multi-Physics Simulation and Experiments in Microelectronics and Micro-Systems. IEEE, pp 1–14

Zhang H, Park S, Hong S (2010) Hygroscopic swelling behavior of molding compound at high temperature. In: 2010 12th IEEE Intersociety Conference on Thermal and Thermomechanical Phenomena in Electronic Systems. IEEE, pp 1–7